
BY NC ND

# Earthquake histories and Holocene acceleration of fault displacement rates

**Andrew Nicol[1], John Walsh[2], Vasiliki Mouslopoulou[2*], and Pilar Villamor[1]**

[1]*GNS Science, PO Box 30368, Lower Hutt, New Zealand*

[2]*Fault Analysis Group, School of Geological Sciences, University College Dublin, Belfield, Dublin 4, Ireland*

[*]Present address: Department of Mineral Resources Engineering, Technical University of Crete, Chania, 73 100, Greece

## ABSTRACT

Displacement rates for normal and reverse faults (N = 57) are generally higher when averaged for the Holocene (~10 ka) than for the late Quaternary (~300 ka) and longer time scales. Holocene acceleration of displacement rates could be attributed to geological processes that produce increases of tectonic tempo. We propose an alternative model in which the observed rate changes arise from variability in earthquake slip and/or recurrence coupled with a sampling bias toward those faults that are best represented at the Earth's surface and accrued displacement fastest during the Holocene. This model is consistent with displacement rates measured over time intervals of up to ~300 k.y. for 129 faults from the Taupo Rift, New Zealand. Departures of earthquake parameters and associated displacement rates from their long-term (>300 k.y.) averages are attributed to fault interactions and occur on time intervals inversely related to these long-term displacement rates and to regional strain rates.

## INTRODUCTION

An increasing body of evidence suggests that faults within many systems may have accrued displacement at faster rates during the Holocene (0–10 ka) than over time intervals of ~300 k.y. or more (e.g., Friedrich et al., 2003; McNeill and Collier, 2004; Roberts and Michetti, 2004; Taylor et al., 2004). This rate increase is supported by the global data set in Figure 1 and has been attributed to a number of mechanisms which increase the frequency and/or size of earthquakes on individual faults. These processes include; climatically induced lithospheric rebound (Hetzel and Hampel, 2005), fault linkage (Taylor et al., 2004) and strain localization (Roberts and Michetti, 2004). There is no evidence to support global Holocene increases of fault linkage or of the rates of plate motion and regional strain accumulation (e.g., Beavan et al., 2002). Similarly, lithospheric rebound driven by deglaciation (and associated regression of Lake Bonneville) (Hetzel and Hampel, 2005), which could account for an increase of displacement rates over the last 10–20 k.y. on some faults in the Basin and Range, may not apply for normal faults in offshore New Zealand and Gulf of Corinth, for example, where deglaciation resulted in sea level rise and lithospheric loading. We therefore propose an alternative explanation in which the observed acceleration of displacement rates during the Holocene reflects temporal variations in earthquake slip and/or recurrence interval arising from fault interactions (e.g., Friedrich et al., 2003; Nicol et al., 2006) coupled with a strong bias toward those faults that are best represented at the Earth's surface. This sampling bias decreases the likelihood of faults with Holocene displacement rates lower than their long-term (≥~300 k.y.) averages being sampled (Fig. 1).

The fault interaction-sampling bias model for Holocene displacement rates higher than the long-term average has been tested using a compilation of displacement rate measurements for 64 faults from a selection of fault systems worldwide, together with constraints from a high quality data set from the active Taupo Rift, which provides a means of analyzing displacements

on 129 faults over time intervals of 2–300 k.y. (Villamor and Berryman, 2001; Taylor et al., 2004; Lamarche et al., 2006; Nicol et al., 2006; Berryman et al., 2008; Canora-Catalán et al., 2008; Mouslopoulou et al., 2008). The Taupo Rift data set is unusually complete and avoids the potential bias that may arise from sampling only a few of the most prominent fault traces in a system. Results from analysis of our multiple fault system data set, augmented by constraints derived from the active faults in the Taupo Rift, have important implications for the variability of earthquake processes.

## TEMPORAL DISPLACEMENT RATE VARIATIONS

Analysis of displacement rate variations on different time scales is achieved using 57 faults from seven normal and reverse fault systems together with a further seven large strike-slip faults (see Figure 1 caption for details). Each fault system includes different numbers of constituent faults that range in size and displacement rates and accommodate different regional strain rates. Comparison of average displacements rates for the Holocene (~10 ka) against average values for the past ~300 k.y. and ≥1 Myr on individual faults, indicates a broad positive correlation, but with the scatter in data suggesting significant variability between the short- and long-term rates (Fig. 1). Despite the scatter in these relations, it is clear that Holocene displacement rates are generally greater than longer-term rates; individual faults usually display ratios of 2–20:1 for short- to long-term values. These differences in rate are too large to be accounted for by uncertainties in the displacement rates which average about ± 35% (Fig. 1 and electronic supplement). Given the diversity in the locations, fault types, regional strain rates, growth histories and displacement rates for the faults in Figure 1, it is possible that the observed acceleration has multiple origins. Our analysis, however, suggests that a single explanation may have widespread application.

The maximum departure of short-term displacement rates from average appears to generally decrease with increasing long-term rates; faster moving faults (e.g., >2–5 mm/yr) have broadly equivalent Holocene and longer-term displacement rates (Fig. 1). As these faster moving faults are generally from areas of high regional strain rates ($>10^{-15}$ $S^{-1}$), strain rate could be an important determinant in the observed data distributions (Fig. 1). A decreased scatter of Holocene displacement rates from their long-term averages for higher strain rate systems could be mainly due to an associated decrease in earthquake recurrence interval (Nicol et al., 2005). For high strain rate fault systems the average recurrence interval is relatively low (e.g., < 2 k.y.) and, as a consequence, variations in displacement rates arising from changes in earthquake recurrence or slip are less likely (than lower strain rate systems) to be reflected in the data averaged over the 10 k.y. Holocene time window. By contrast, for faults within low strain rate systems, recurrence intervals will approach, or may even exceed, the 10 k.y. Holocene time window, and short-term displacement rates could be high because they do not sample an entire recurrence interval.

## TAUPO RIFT FAULTS

In an attempt to provide a rationale for the higher than average Holocene displacement rates of Figure 1, high quality displacement and paleoearthquake data are presented for 129 normal faults from the Taupo Rift (North Island of New Zealand), that range in length (1–70 km), displacement rate (0.01–4 mm/yr) and topographic scarp height (0.3–150 m). Displacement rates together with the timing and slip of paleoearthquakes have been determined for parts of the rift, which is a back-arc basin extending at rates up to ~12 mm/yr across a width of 15–30 km (Villamor and Berryman, 2001; Wallace et al., 2004). What distinguishes the Taupo Rift data set from others, are the exceptional quantitative constraints on fault displacement accumulation, for

93 all major faults in the system and for a range of time scales, which derive from a combination of
94 the full range of conventional paleoseismological methods and geophysical tools (Villamor and
95 Berryman, 2001; Lamarche et al., 2006; Nicol et al., 2006; Berryman et al., 2008; Canora-
96 Catalán, et al., 2008; Mouslopoulou et al., 2008).

97 Displacement rates on faults from the Taupo Rift have an approximately proportional
98 positive relation with fault length, for time intervals of 10 k.y. and greater (Fig. 2). This increase
99 in displacement rate with fault size is similar to other fault systems and confirms that longer
100 faults generally move faster than short (Nicol et al., 2005; Mouslopoulou et al., 2009). The
101 positive correlation has been attributed to the proportional relation between earthquake slip and
102 fault length, with the y-axis value increasing for higher regional strain rates (Nicol et al., 2005;
103 Mouslopoulou et al., 2009). An additional important feature of Figure 2 is the progressive
104 increase in scatter of displacement rates for shorter time scales. The increase in scatter, in
105 combination with displacement profiles for faults in the Taupo Rift for the last 26 k.y. (Nicol et
106 al., 2006), support the notion that individual faults can experience short-term variations in
107 displacement rates and that, while time intervals of accelerated displacement accumulation are
108 common in the Taupo Rift, these variations are generally not synchronous on individual faults
109 and certainly not confined to the Holocene. During the Holocene, faults in the Taupo Rift have
110 displacement rates faster, slower and approximately equal to the long-term average rates
111 measured over time periods of ≥ 60 k.y. (Fig. 2).

112 The question is why some systems, such as the Taupo Rift, do not show a bias toward
113 higher rates on 10 k.y. time intervals while others do? Examination of short-term displacement
114 rates on the Taupo Rift faults indicate that for 2 k.y. intervals faults have approximately bimodal
115 displacement rates, i.e., they generally have higher than average displacement rates or, within

resolution, they do not move at all (Fig. 2). This feature is consistent with the fact that estimates of the recurrence interval of large earthquakes on individual faults in Taupo Rift are ~2–3 k.y. (Nicol et al., 2005). The significant number of higher than average displacement rate faults over the past 2 k.y. in Taupo Rift (0-2 k.y. in Fig. 2), partly arises because measurements derive from trenches which were generally located on the most clearly defined fault scarps. The smaller proportion of low displacement rate faults, sometimes characterized by no discernible displacement over the measured period, are not as easily identified and are therefore less often sampled. While fault-scarp preservation potential is dependent on the relative rates of fault slip and sedimentation (or burial), within a given system (i.e., where rates of surface processes are comparable on all faults) faults which have ruptured most recently tend to have the best preserved scarps and are more likely to have rates that are higher than their long-term averages.

The lack of sampling bias toward those Taupo Rift faults which have moved fastest in the Holocene is mainly because the available data are of extremely high quality and the ~10 k.y. sample window by far exceeds the average earthquake recurrence interval (~2–3 k.y.). While the ~10 k.y. displacement rates measured are broadly representative of the long-term rates, they nevertheless still display about one order of magnitude of scatter, even when sampled at time scales approaching five times the average recurrence interval, a feature which reflects significant variability in earthquake slip and/or recurrence interval. The observed Taupo Rift data distributions demonstrate that, for time scales approaching, or shorter than, the average recurrence interval of faults, sampling biases will result in higher than average displacement rates even for very high quality data sets such as those of the Taupo Rift.

## IMPLICATIONS FOR EARTHQUAKE PROCESSES

Figures 1 and 2 suggest that many faults experience short-term displacement rates that differ from their long-term average. Temporal variations in displacement rates in the Taupo Rift, particularly on timescales of 10 k.y. or less, are accompanied by changes in earthquake slip and recurrence interval, which in both cases exceed an order of magnitude (e.g., Fig. 3). Similar variations in earthquake recurrence intervals on individual faults have been widely observed (e.g., Wallace 1987; Marco et al., 1996; Friedrich et al., 2003; Palumbo et al., 2004; Weldon et al., 2004), while evidence of variable slip per event through time is beginning to emerge but is less commonly reported (e.g., Palumbo et al., 2004; Weldon et al., 2004; Canora-Catalán et al., 2008). Collectively, paleoearthquake studies show that it is these changes in earthquake parameters for consecutive events on individual faults that produce variability in fault displacement rates. This assertion is supported by the complex form of displacement-time curves for individual faults in the Taupo and Taranaki rifts in New Zealand, which are directly linked to the variable displacement rates (Nicol et al., 2006; Mouslopoulou et al., 2009).

The link between displacement rates and earthquake parameters is shown by the displacement-time curve in Figure 4. This synthetic curve was generated using Taupo Rift earthquake data from multiple faults by randomly choosing pairs of recurrence intervals and slip/event from the population of paleoearthquakes on 0–0.3 mm/yr faults shown in Figure 3. Though such a simple stochastic model does not contain any conditioning, the displacement-time curve nevertheless produces average displacement rates for 10 k.y. time intervals which range from 0 to 0.5 mm/yr, a variability similar to that of 5–10 km long faults in Figure 2. This model provides an indication of how changes in earthquake slip and recurrence can influence fault displacement rates, while the resulting displacement-time curve supports the notion that complex

earthquake behavior is an intrinsic property of fault systems and is a critical determinant on the variability of displacement rates.

There are insufficient data to define the precise geometries of displacement-time curves, although Figures 1–2 and previous work (e.g., Wallace, 1987; Palumbo et al., 2004; Weldon et al., 2004; Nicol et al., 2006) indicate that the nonlinearity depicted in Figure 4 is common. In such cases the time- and slip-predictable earthquake models (e.g., Shimazaki and Nakata, 1980) can, at best, only apply for part of a fault's history. The minimum length of time required to measure representative long-term displacement rates provides an estimate of the timescales of displacement rate variations on individual faults (e.g., Fig. 4). Displacement rates comparable to long-term values occur on time intervals as short as ~1–2, 10 and 20–60 k.y. for the 20–30 mm/yr San Andreas fault at Wrightwood (Weldon et al., 2004), the ~2–5 mm/yr faults in Figure 1 (this study) and the <1 mm/yr Taupo Rift faults (Nicol et al., 2006), respectively. The inverse relation between displacement rate (and regional strain rate) and these time intervals derives from the reduction of average recurrence interval with increasing displacement rate (e.g., the San Andreas fault at Wrightwood has an average recurrence of ~100 yr and the Taupo Rift faults ~2–3 k.y.).

Many processes could contribute to the observed order of magnitude changes in displacement rate and earthquake slip and recurrence (e.g., Figures 3 and 4), including temporal changes in fault strength, fault segmentation, fault healing rate, fault loading rate and fault interactions (e.g., Wallace, 1987; Friedrich et al., 2003; Weldon et al., 2004). The uniformity of the driving plate motions and the constant regional strain rates on timescales of tens of thousands of years in some fault systems indicate that, in these cases, variations in earthquake slip and recurrence arise from processes within the fault systems themselves rather than from changes in

their boundary conditions. Static stress modeling of fault systems shows that fault interactions can produce variations in the rates of strain release (i.e., earthquake slip and/or recurrence intervals) even when the fault strength, fault loading rates and stored stresses are approximately uniform (e.g, Robinson, 2004). A corollary of the fault interaction model is that fault systems which comprise fewer faults in relatively simple configurations, such as parts of some large strike-slip fault systems (e.g., North Anatolian and Alpine fault systems), would be expected to show less complexity in their earthquake behavior than faults in systems that comprise many interacting components.

**ACKNOWLEDGEMENTS**

This research was funded by the Marsden Fund and FRST in New Zealand, an IRCSET Embark Post-Doctoral Fellowship and by a UCD (Ireland) President's Fellowship. We thank Richard Norris and an anonymous reviewer for helpful and constructive reviews.

**REFERENCES CITED**

Beavan, J., Tregoning, P., Bevis, M., Kato, T., and Meertens, C., 2002, The motion and rigidity of the Pacific Plate and implications for plate boundary deformation: Journal of Geophysical Research, v. 107, p. 2261, doi:10.1029/2001JB000282.

Berryman, K., Villamor, P., Nairn, I., Van Dissen, R., Begg, J., and Lee, J., 2008, Late Pleistocene surface rupture history of the Paeroa Fault, Taupo Rift, New Zealand: New Zealand Journal of Geology and Geophysics, v. 51, p. 135–158.

Canora-Catalán, C., Villamor, P., Berryman, K., Martínez-Diaz, J.J., and Raen, T., 2008, Rupture history of the Whirinaki Fault, an active normal fault in the Taupo Rift, New Zealand: New Zealand Journal of Geology and Geophysics, v. 51, p. 277–293.

Friedrich, A.M., Wernicke, B.P., Niemi, N.A., Bennett, R.A., and Davis, J.L., 2003, 2003, Comparison of geodetic and geologic data from the Wasatch region, Utah, and implications for the spectral character of Earth deformation at periods of 10 to 10 million years: Journal of Geophysical Research, v. 108, no. B4, p. 2199, doi: 10.1029/2001JB000682.

Hetzel, R., and Hampel, A., 2005, Slip rate variations on normal faults during glacial-interglacial changes in surface loads: Nature, v. 435, p. 81–84, doi: 10.1038/nature03562.

Lamarche, G., Barnes, P.M., and Bull, J.M., 2006, Faulting and extension rate over the last 20,000 years in the offshore Whakatane Graben, New Zealand continental shelf: Tectonics, v. 25, p. TC4005, doi: 10.1029/2005TC001886.

Marco, S., Stein, M., and Agnon, A., 1996, Long-term earthquake clustering: A 50,000-year paleoseismic record in the Dead Sea Graben: Journal of Geophysical Research, v. 101, B3, p. 6179–6191, doi: 10.1029/95JB01587.

McNeill, L.C., and Collier, R.E.L., 2004, Uplift and slip rates of the eastern Eliki fault segment, Gulf of Corinth, Greece, inferred from Holocene and Pleistocene terraces: Journal of the Geological Society, v. 161, p. 81–92, doi: 10.1144/0016-764903-029.

Mouslopoulou, V., Nicol, A., Walsh, J.J., Beetham, D., and Stagpoole, V., 2008, Quaternary temporal stability of a regional strike-slip and rift fault intersection: Journal of Structural Geology, v. 30, p. 451–463, doi: 10.1016/j.jsg.2007.12.005.

225 Mouslopoulou, V., Walsh, J.J., and Nicol, A., 2009, Fault displacement rates on a range of
226 timescales. Earth and Planetary Science Letters, v. 278, p. 186-197,
227 doi:10.1016/j.epsl.2008.11.031 .
228 Nicol, A., Walsh, J.J., Manzocchi, T., and Morewood, N., 2005, Displacement rates and average
229 earthquake recurrence intervals on normal faults: Journal of Structural Geology, v. 27,
230 p. 541–551, doi: 10.1016/j.jsg.2004.10.009.
231 Nicol, A., Walsh, J.J., Berryman, K., and Villamor, P., 2006, Interdependence of fault
232 displacement rates and paleoearthquakes in an active rift: Geology, v. 34, p. 865–868, doi:
233 10.1130/G22335.1.
234 Palumbo, L., Benedetti, L., Bourles, D., Cinque, A., and Finkel, R., 2004, Slip history of the
235 Magnola fault (Appennines, Central Italy) from $^{36}$Cl surface exposure dating: evidence for
236 strong earthquakes over the Holocene: Earth and Planetary Science Letters, v. 225, p. 163–
237 176, doi: 10.1016/j.epsl.2004.06.012.
238 Roberts, G.P., and Michetti, A.M., 2004, Spatial and temporal variations in growth rates along
239 active fault systems: an example from Lazio-Abtuzzo, central Italy: Journal of Structural
240 Geology, v. 26, p. 339–376, doi: 10.1016/S0191-8141(03)00103-2.
241 Robinson, R., 2004, Potential earthquake triggering in a complex fault network: the northern
242 South Island, New Zealand: Geophysical Journal International, v. 159, p. 734–748, doi:
243 10.1111/j.1365-246X.2004.02446.x.
244 Shimazaki, K., and Nakata, T., 1980, Time-predictable recurrence model for large earthquakes:
245 Geophysical Research Letters, v. 7, no. 4, p. 279–282, doi: 10.1029/GL007i004p00279.

246 Taylor, S.K., Bull, J.M., Lamarche, G., and Barnes, P.M., 2004, Normal fault growth and linkage
247 in the Whakatane Graben, New Zealand, during the last 1.3 Myr. Journal of Geophysical
248 Research, 109, B2, B02408, doi:10.1029/2003JB002412.
249 Villamor, P., and Berryman, K., 2001, A late Quaternary extension rate in the Taupo Volcanic
250 Zone, New Zealand, derived from fault slip data: New Zealand Journal of Geology and
251 Geophysics, v. 44, p. 243–269.
252 Wallace, L., Beavan, J., McCaffrey, R., and Darby, D., 2004, Subduction zone coupling and
253 tectonic block rotation in the North Island, New Zealand: Journal of Geophysical Research,
254 v. 109, no. B12, doi: 10.1029/2004JB003241.
255 Wallace, R.E., 1987, Grouping and migration of surface faulting and variations in slip rates on
256 faults in the Great Basin Province: Bulletin of the Seismological Society of America, v. 77,
257 p. 868–876.
258 Weldon, R., Scharer, K., Fumal, T., and Biasi, G., 2004, Wrightwood and the earthquake cycle:
259 what a long recurrence record tells us about how faults work: GSA Today, v. 14, doi:
260 10.1130/1052-5173(2004)014<4:WATECW>2.0.CO;2.

261 **FIGURE CAPTIONS**

262 Figure 1. Comparison of displacement rates averaged over the Holocene (~10 k.y.) with average
263 values for the million year (≥1 Myr) (A) and Late Quaternary (~300 k.y.) (B) time intervals
264 using a global data set of 65 faults. The names, locations (country and fault system), fault types,
265 displacement rates (and their uncertainties) and data sources for the faults are given in the
266 electronic supplement. The faults have a range of sizes, with lengths of 10–700 km and total
267 displacements of up to ~315 km, and slip rates of ~0.01–30 mm/yr. Symbols are as follows:
268 unfilled triangle, strike-slip (San Andreas, Alpine, Dead Sea Transform, North Anatolian,

269 Awatere, Sumatra and Itoilawa Shizuoku tectonic line faults); unfilled diamond, Taupo Rift
270 (normal faults); unfilled circle, Corinth Rift (normal faults); unfilled square, Apennines (normal
271 faults); filled triangle, New Zealand Hikurangi margin (reverse faults); filled diamond Taranaki
272 Rift (normal faults); filled circle Wanganui Basin (reverse and normal faults) and filled square,
273 Basin and Range (normal faults). Regional strain rates are greater or less than $10^{-15}$ $S^{-1}$ for
274 unfilled and filled faults, respectively. Contours of the Holocene/Late Quaternary or Myr
275 displacement rate ratios are illustrated.
276 Figure 2. Taupo Rift displacement rate vs fault length for sample intervals of 2, 10, 60 and 300
277 k.y. Displacement histories for normal faults have been charted for volcanic horizons ranging in
278 age from 2 to 300 k.y. (e.g., Villamor and Berryman, 2001) using displacements from trenches (2
279 and 10 k.y.), topographic scarp heights (10, 60 and 300 k.y.), and seismic reflection lines and
280 outcrop (300 k.y.) (e.g., Villamor and Berryman, 2001; Nicol et al., 2006; Lamarche et al., 2006;
281 Berryman et al., 2008; Mousloupolou et al., 2008). Data for the last 2 k.y. (~0-2 ka, solid blue
282 squares) and older 2 k.y. (~2 ka, open blue squares) sample intervals are discriminated.
283 Horizontal dashed lines labeled 2 k.y. RL and 10 k.y. RL indicate the lower resolution limit of
284 displacement rate for 2 and 10 k.y. data respectively.
285 Figure 3. Plot illustrating variations in excess of one order of magnitude of earthquake slip/event
286 and recurrence intervals for consecutive paleoearthquakes recorded in trenches across 26
287 individual faults in the Taupo Rift (e.g., Berryman et al., 2008). Displacements for up to 13
288 volcanic tephra and fluvial sediment layers in each trench record as many as seven surface-
289 rupturing paleoearthquakes (~Mw 5.8–6.8) on each fault over the last ~26 k.y. (Villamor and
290 Berryman, 2001; Nicol et al., 2006; Berryman et al., 2008). Slip/event and recurrence intervals of
291 less than 0.1–0.3 m and 1–2 k.y., respectively, are sub-resolution and while their inclusion may

modify the recurrence and slip populations, they are unlikely to entirely remove the variability of these earthquake parameters. Slip/event and recurrence intervals with a common long-term (~60 k.y.) displacement rate indicate different earthquakes on the same fault..

Figure 4. Stochastic displacement-time profile for a notional normal fault with a long-term displacement rate of ~0.14 mm/yr and total displacement of 27.2 m produced in 31 earthquakes over 200 k.y. Profile constructed by randomly sampling recurrence interval and slip/event pairs from the paleoearthquake distribution for those faults in Figure 3 with long-term displacement rates of 0–0.3 mm/yr. Grey smoothed curve is a running average of 10 k.y. sample intervals. Numbers above rectangles indicate average displacement rates for selected 10 k.y. time intervals.

[1]GSA Data Repository item 2009xxx, xxxxxxxx, is available online at www.geosociety.org/pubs/ft2008.htm, or on request from editing@geosociety.org or Documents Secretary, GSA, P.O. Box 9140, Boulder, CO 80301, USA.

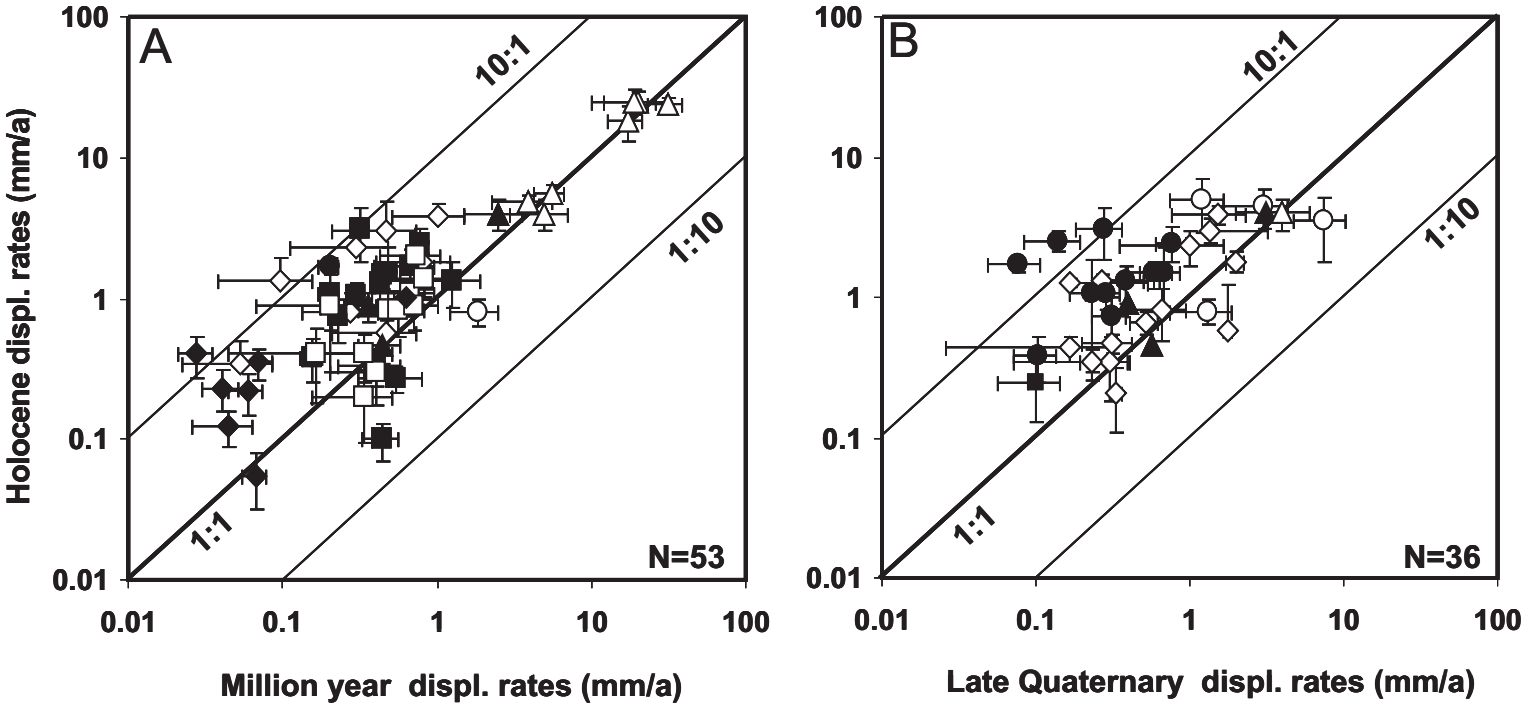
A
B
10:1
1:1
1:10
N=53
N=36
100
10
1
0.1
0.01
Holocene displ. rates (mm/a)
Million year displ. rates (mm/a)
Late Quaternary displ. rates (mm/a)

Figure 1

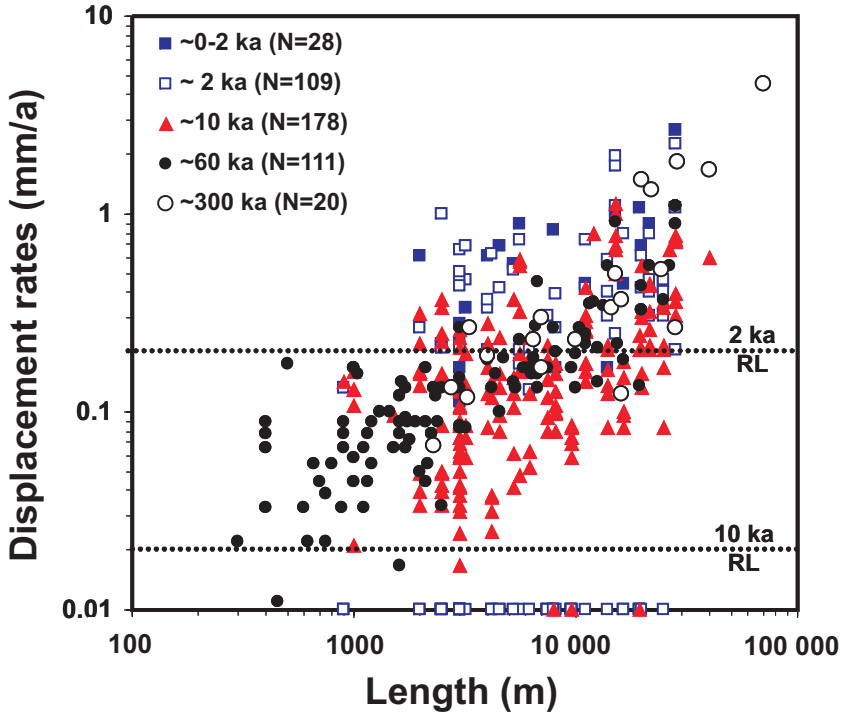
10
1
0.1
0.01
Displacement rates (mm/a)
~0-2 ka (N=28)
~ 2 ka (N=109)
~10 ka (N=178)
~60 ka (N=111)
~300 ka (N=20)
2 ka RL
10 ka RL
100
1000
10 000
100 000
Length (m)

**Figure 2**

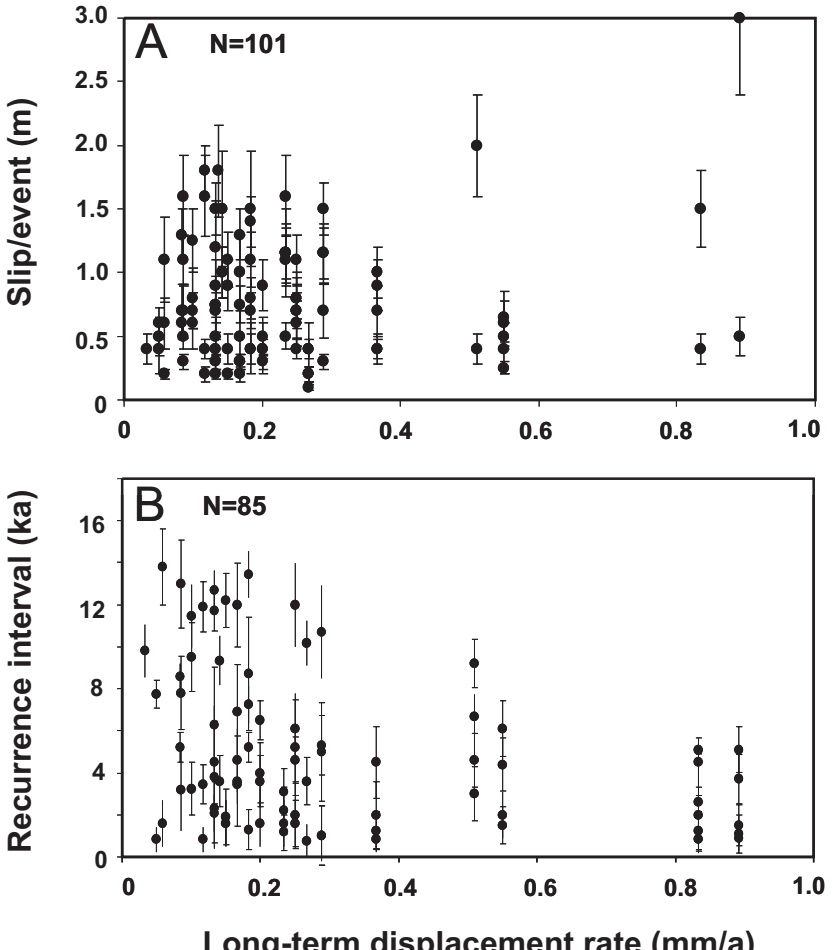
A
N=101
Slip/event (m)
3.0
2.5
2.0
1.5
1.0
0.5
0
0
0.2
0.4
0.6
0.8
1.0
B
N=85
Recurrence interval (ka)
16
12
8
4
0
0
0.2
0.4
0.6
0.8
1.0
Long-term displacement rate (mm/a)

Figure 3

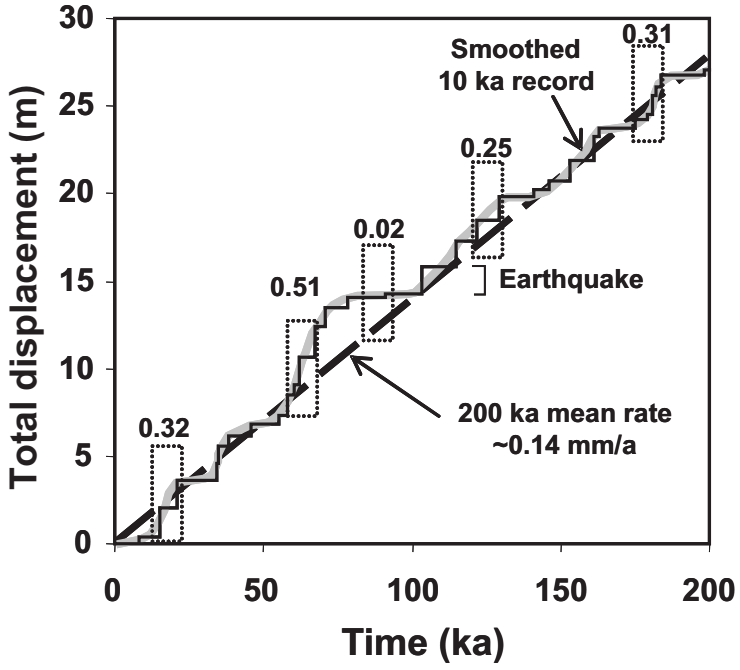
Total displacement (m)
Time (ka)
0
5
10
15
20
25
30
0
50
100
150
200
0.32
0.51
0.02
0.25
0.31
Smoothed
10 ka record
Earthquake
200 ka mean rate
~0.14 mm/a

Figure 4